Research Article

Maalee Almheidat, Zeeshan*, Ali Althobaiti, Naveed Iqbal, Ali M. Mahnashi, and Rasool Shah

Reliability of two-dimensional steady magnetized Jeffery fluid over shrinking sheet with chemical effect

https://doi.org/10.1515/phys-2024-0076
received February 29, 2024; accepted July 30, 2024

Abstract: A numerical framework is established for a two-dimensional steady flow of the magnetized Jeffery fluid model over elongated/shrinking sheets, with potential applications such as coating sheets, food products, fiber optics, drilling fluids, and the manufacturing processes of thermoplastic polymers. The model also demonstrates the influence of chemical reaction, magnetic field, and stability analysis which provide a novel contribution to this study. To ensure the ease and effectiveness of this analysis, we transform the set of difference equations governing the system into ordinary equations using the similarity transformation. The reliability of the solution is examined by using stability analysis. The Navier–Stokes equations have been transformed into self-similar equations by adopting appropriate similarity transformations and subsequently solved numerically using the bvp4c (three-stage Labatto-three-A formula) approach. The comparison between the derived asymptotic solutions and previously documented numerical results is quite remarkable. The self-similar equations display a duality of solutions within a limited range of the shrinking parameter, as observed from the data. For each stretching scenario, there is a unique solution. Hence, an examination of temporal stability has been conducted through linear analysis to establish the most fundamentally viable solution. The determination of stability in the analysis is based on the sign of the smallest eigenvalue, which indicates whether a solution is unstable or stable. The analysis of stability reveals that the first solution, which describes the primary flow, remains stable. Through the utilization of graphs, we thoroughly examine and discuss the influence of emerging factors. The numerical results obtained from this analysis demonstrate multiple solutions within a certain range of $M_1 \geq M_{ci}$, $i = 1, 2, 3$, and no solution in the range $M_1 < M_{ci}$. M_{ci} denotes the critical values, which increase as the quantities of Sc increase from 0.3 to 0.9. Similarly, multiple solutions exist for $\lambda \geq \lambda_{ci}$, $i = 1, 2, 3$, and no solution in the range $\lambda < \lambda_{ci}$ is observed.

Keywords: multiple solutions, chemical reaction, magnetized Jeffery fluid model, shrinking sheet

1 Introduction

The field of technical and materials science has witnessed a surge in interest toward non-Newtonian materials in recent decades. The occurrence of non-Newtonian behavior can be observed in various applications, such as coating sheets, food products, fiber optics, drilling fluids, and the manufacturing processes of thermoplastic polymers. Among the various fluid models, the Jeffrey liquid serves as a noteworthy exemplification, engrossing the attention and inquisitiveness of numerous researchers. It is noteworthy to mention that this particular flow model is characterized by the occurrence of relaxing and delayed reactions, which have the potential to unveil a plethora of novel insights and knowledge. The practical implications of this are far-reaching, as a comprehensive understanding of the Jeffrey liquid can be leveraged to optimize extrusion operations, crystal and sheet manufacturing processes, semiconductor circuitry, crystal growth, and a multitude of other fields, all of which stand to reap tremendous benefits from the study of boundary layer movements over a stretching cylinder [1]. Sun *et al.* [2] studied the Casson

* **Corresponding author: Zeeshan,** Department of Mathematics and Statistics, Bacha Khan University Charsadda, Charsadda, KP, Pakistan, e-mail: zeeshan@bkuc.edu.pk
Maalee Almheidat: Department of Mathematics, University of Petra, Amman, 11196, Jordan, e-mail: malmheidat@uop.edu.jo
Ali Althobaiti: Department of Mathematics, College of Science, Taif University, P.O. Box 11099, Taif, 21944, Saudi Arabia, e-mail: aa.althobaiti@tu.edu.sa
Naveed Iqbal: Department of Mathematics, College of Science, University of Ha'il, Ha'il, 2440, Saudi Arabia, e-mail: n.iqbal@uoh.edu.sa
Ali M. Mahnashi: Department of Mathematics, Faculty of Science, Jazan University, P.O. Box 2097, Jazan, 45142, Saudi Arabia, e-mail: amahnashi@jazanu.edu.sa
Rasool Shah: Department of Computer Science and Mathematics, Lebanese American University, Beirut, Lebanon

boundary layer movement over the wedge sheet. Krishna *et al.* [3] gave a comparison of Skiadis and Blasius magnetized flow with thermal effects and varying properties. Significant advances in this sector have been highlighted in recent articles [4–10], opening the door for optimization in a variety of industrial processes.

It should be noted that most of the studies that have been done up to this point have mostly concentrated on the flows that are caused by a surface that is extended vertically. This specific feature has emerged repeatedly in the previously described research. However, it is essential to recognize that several research studies [11–15] have also looked at various aspects of this phenomenon. These investigations have covered a wide range of topics related to the flows caused by a stretched surface, which has resulted in a deeper understanding of the topic. Through their recent investigation of magnetized viscous fluid flow on probabilistic extending surfaces in the setting of a chemical process, Raptis and Perdikis [16] have contributed significant improvements to the domain. Their inquiry is primarily focused on achieving two basic goals. First of all, by analyzing the behavior of Jeffrey liquids, they want to improve the present knowledge of flow properties [16].

Magnetohydrodynamics, the study of the magnetism of electrically conducting materials, has found widespread use in a wide range of fields, from chemical manufacturing to transport engine cooling systems, electronic chip cooling, plasma, nuclear-powered sector, saltwater, *etc.* It is used in the disciplines of metalworking and polymer engineering. Potential magnetohydrodynamics (MHD) uses include magnetic drug targeting, astronomical sensing, and architecture [17,18]. Particularly, MHD plays a crucial character in star development. Given these substantial advantages, researchers and statisticians continuously analyze MHD flows. Chu *et al.* [19] reported the numerical results for Jeffrey fluid-suspended nanomaterials with chemical response over parallel disks. Lund *et al.* [20] displayed the stability assessment of hybrid nanofluid propagating over a time-dependent extended sheet with a slip effect. Khan *et al.* [21] studied the magnetic effect in Ree-Eyring nanomaterial across a stretching sheet. Souayeh *et al.* [22] investigated the magnetic dipole movement with a heat source across an extended sheet. Similarly, Souayeh [23] explored the characteristics of the CC-heat flux of ternary nanofluid with Lorentz force and slip effects.

Despite the substantial importance and frequent occurrence of non-Newtonian phenomena in various sectors and technological domains, there is a significant dearth of prior scholarly publications addressing the flow characteristics of a magnetized non-Newtonian Jeffery fluid over a stretching or shrinking surface with stability analysis. The primary objective of the present investigation is to bridge this gap in the existing corpus of knowledge. In order to accomplish this, the current study employs the Jeffery fluid model as the foundational framework for the flow analysis. Moreover, the fluid being demonstrates electrical conductivity when a uniform magnetic field is present, and the stability of the model adds a new aspect to the analysis. Furthermore, the investigation also takes into consideration the presence of chemically reactive constituents within the flow field, thereby expanding the scope of the study to encompass the intricate interplay between fluid dynamics and chemical reactions. The present study is organized as follows: Section 2 represents the mathematical formulation, Section 3 signifies the numerical procedure and validation of code, and Section 4 provides the results and discussion of the model.

2 Mathematical analysis

Consider steady, two-dimensional, and incompressible MHD flow Jeffery fluid across an extended and contracting sheet. The sheet is stretched or contracted with velocity: $U_w = \lambda_1(a_1x + b_1x^2)$, where λ_1 is elongating ($\lambda_1 > 0$) and contracting ($\lambda_1 < 0$) sheet variable. For the purpose of this analysis, a coordinate system is selected, denoted by (x, y), where the x-axis is aligned with the stretching or shrinking surface, while the y-axis is perpendicular to it. It is crucial to acknowledge that a consistent magnetic field is present in the y-direction, giving rise to further intricacies in the flow dynamics.

The leading flow equations for continuity and temperature are [9,12,14]

$$\frac{\partial u}{\partial x} + \frac{\partial v}{\partial y} = 0, \tag{1}$$

$$u\frac{\partial u}{\partial x} + v\frac{\partial v}{\partial y} + \omega_1\left(u^2\frac{\partial^2 u}{\partial x^2} + v^2\frac{\partial^2 u}{\partial y^2} + 2uvu^2\frac{\partial^2 u}{\partial x \partial y}\right) = v\left(\frac{\partial^2 u}{\partial y^2} + \omega_2\left(\left(\frac{\partial^2 u}{\partial x \partial y^2} + v\frac{\partial^3 u}{\partial y^3} - \frac{\partial u}{\partial x}\frac{\partial^2 u}{\partial y^2} - \frac{\partial u}{\partial x}\frac{\partial^2 v}{\partial y^2}\right)\right)\right) - \frac{\sigma B_0^2}{\rho}, \tag{2}$$

$$u\frac{\partial C}{\partial x} + v\frac{\partial C}{\partial y} - D\frac{\partial^2 C}{\partial y^2} - RC = 0, \tag{3}$$

In Eqs. (1)–(3), u and v are velocity components along x- and y-directions, ν is the dynamic viscosity, ρ is the fluid density, σ is the thermal conductivity, ω_1 and ω_2 are the relaxation/retardation parameters, C is the concentration, D is the diffusion factor, and R is the reaction parameter.

Boundary conditions for the present problem are [9,10]

$$u(x,y) = U_w = \lambda_1(a_1x + b_1x^2),\ v(x,y) = 0,\quad C(x,y) = C_w, \text{ at } y = 0, \tag{4}$$

$$u \to 0, C \to 0, y \to \infty, \tag{5}$$

where $a_1,\ b_1$ in Eq. (4) are constants.

Using the following suitable transformation variables:

$$\begin{aligned}
\eta &= \left(\frac{a_1}{\nu}\right)^{1/2} y,\\
u &= a_1 x f'(\eta) + b_1 x^2 g'(\eta),\\
v &= -(a_1\nu)^{1/2} f(\eta) - 2b_1 x\left(\frac{\nu}{a_1}\right)^{1/2} g(\eta),\\
C &= C_w\left(C_0(\eta) + \frac{2xb_1}{a_1}C_1(\eta)\right).
\end{aligned} \tag{6}$$

Using Eq. (6) in Eqs. (2)–(5), we obtain

$$\begin{aligned}
&f''' + M^2 f' - (f')^2 + ff''\\
&+ \Omega_1(2ff'f'' - f^2 f''') + \Omega_2((f'')^2 - ff'''') = 0,
\end{aligned} \tag{7}$$

$$\begin{aligned}
&g'''' + M^2 f' - 3f'g' + 2gf'' + f'g''\\
&+ \Omega_1(4ff'g'' + 2ff'' - f^2 g'' - 4fgf'' + 4f'gf'' - 2f^2 g')\\
&+ \Omega_2(f'g'' - g'f''' - fg'''' - 2gf'''' + 3f''g'') = 0,
\end{aligned} \tag{8}$$

$$C_0'' + \mathrm{Sc} f C_0' - \mathrm{Sc}\gamma C_0 = 0, \tag{9}$$

$$C_1'' + \mathrm{Sc} f C_1' - \mathrm{Sc} f' C_1 - \mathrm{Sc}\gamma C_1 + \mathrm{Sc} g C_0' = 0. \tag{10}$$

With

$$\begin{aligned}
&f = 0, f' = \lambda_1, g = 0, g' = 1, \quad C_0 = 1, C_1 = 0; \text{ at } \eta \to 0,\\
&f' = 0.\ g' = 0, C_0 = 1, C_1 = 0, \text{ at } \eta \to \infty.
\end{aligned} \tag{11}$$

In the above equations, $\gamma(=\frac{R}{a_1})$ is the reaction rate parameter, $\mathrm{Sc}(=\frac{\nu}{D})$ is the Schmidt number, $M(=\frac{\sigma B_0^2}{a_1\rho})$ is the magnetic factors, and $\Omega_1(=\omega_1 a_1)$, $\Omega_2(=\omega_2 a_1)$ are the Deborah numbers.

Mathematical expressions for mass transportation at the surface are

$$\begin{aligned}
C_0'(0) &= \left(\frac{\partial C_0}{\partial \eta}\right)_{\eta=0} \le 0,\\
C_1'(0) &= \left(\frac{\partial C_1}{\partial \eta}\right)_{\eta=0} \le 0.
\end{aligned} \tag{12}$$

3 Numerical procedure and validation of code

Nonlinear ordinary differential equations (ODEs) with specific conditions cannot be addressed through analytical means (Eqs. (6)–(9) with constraints (10)). In order to solve differential equations of this nature, computational methods are necessary. The existing literature provides various numerical techniques, among which the bvp4c technique proves to be particularly useful for solving first-order initial value problems (IVPs). Therefore, we employed the bvp4c method to solve the aforementioned system. The bvp4c method is a finite-difference code that utilizes the three-stage Labatto IIIa formula. Generally, it adopts a collocation approach with fourth-order accuracy over the integrated time frame of the computation. The residual of the ongoing solution is utilized to facilitate error prevention and mesh selection in this case. An approximate tolerance level of 10^{-6} was established. Given that this problem encompasses multiple solutions, an "excellent" initial estimation is necessary to obtain an accurate solution. This estimation should satisfy the provided boundary constraints and reflect the nature of the solution. Despite the availability of initial predictions, the bvp4c approach primarily converges to the first solution, thus simplifying the discovery of the first solution. However, accurately estimating the second solution for the extension of a sheet when $\lambda < 0$ proves to be more challenging. The methodology known as "continuation" is extensively discussed in the book by Shampine *et al.* [24]. This technique involves substituting the "infinity" at Eq. (11) with a finite quantity that is determined by the numerical values of the relevant parameters. To ensure convergence, we initiate the process with a small value (*e.g.*, $\eta = \eta\infty = 5$) and gradually increase it until convergence is achieved. The finite value chosen for $\eta \to \infty$ is $\eta_\infty = 7$ for both the first and second solutions. The visual representation of the bvp4c is presented in Figure 1.

For validation of the current study, it is compared with the published work for surface mass transfer (SMTr) using various values of Sc = 0.1, 0.3, 0.6, 0.9, 1.1, γ = 0.1, 0.3, 0.5, 0.7, 1.1, M = 0.2, 0.4, 0,6, 0.8, 1.2, and $\Omega_1 = \Omega_1$ = 0.1, 0.3, 0.5, 0.9, and 1.1. This depicts that the values mass transfer at the surface $-C_0'(0)$ increases as the magnitude of Sc, Y, and $\Omega_1 = \Omega_2$ are improved, whereas declines for growing of M from 0.1 to 1.5. Likewise, the magnitude of $-C_1'(0)$ improves with the growing values of Sc, M, and $\Omega_1 = \Omega_2$ and diminishes for large values of Y growing from 0.2 to 1.5. For the ratification of the existing work scheming, the obtainable results are also associated with distributed work described by Tasawar *et al.* [25] for SMTr $-T_0'(0)$ and $-T_1'(0)$, and an admirable settlement is established, as exposed in Table 1.

4 Results and discussion

This research focuses on studying the mixed convection movement of a Jeffrey non-Newtonian fluid across a

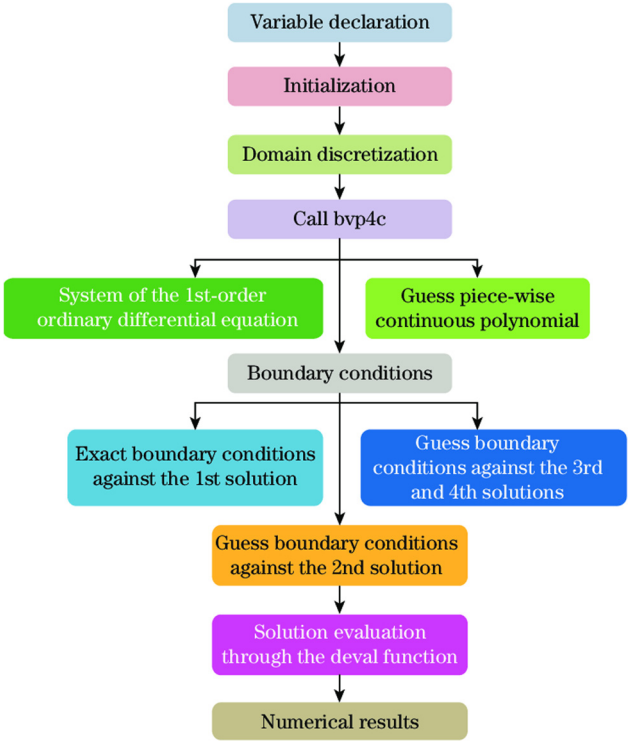

Figure 1: Flow chart of the numerical scheme.

surface that is simultaneously contracting and stretching while being subjected to an electromagnetic field. The issue

Table 1: Comparison of the variation of surface mass transfer $-T_0'(0)$ and $-T_1'(0)$ for some values of Sc, Y, M $\Omega_1 = \Omega_2$ with published work explored by Tasawar *et al.* [25]

Sc	Y	M	$\Omega_1 = \Omega_2$	$-T_0'(0)$	$-T_1'(0)$	Tasawar *et al.* [25] $-T_0'(0)$	Tasawar *et al.* [25] $-T_1'(0)$
1	0.1	0.1	0.3	0.83401	0.15635	0.83412	0.15646
	0.3			1.05812	0.13301	1.05823	0.13321
	0.5			1.15247	0.12571	1.15258	0.12582
	0.7			1.53462	0.10361	1.53473	0.10372
0.1	1.1			0.79830	0.07516	0.79841	0.07527
0.3				0.87932	0.08642	0.87943	0.08653
0.6				1.42747	0.16652	1.42758	0.16663
0.9				1.66063	0.20160	1.66074	0.20171
1.1	1.2	0.1		1.17762	0.12354	1.17773	0.12365
		0.2		1.17543	0.12405	1.17554	0.12416
		0.4		1.16955	0.12515	1.16966	0.12526
		0.6		1.16142	0.12600	1.16153	0.12605
		0.8		1.15247	0.12572	1.15258	0.12583
		1.1	0.1	1.14837	0.11830	1.14848	0.11841
			0.3	1.15247	0.12571	1.15258	0.12582
			0.5	1.55647	0.12981	1.55658	0.12992
			0.9	1.16018	0.13372	1.16029	0.13383
			1.1	1.16212	0.13458	1.16204	0.13469

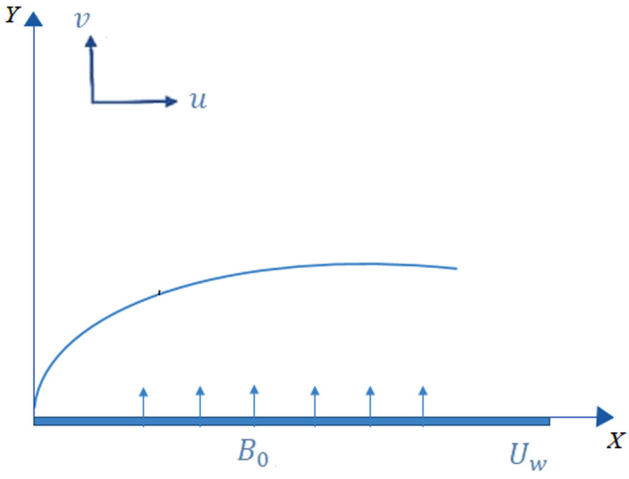

Figure 2: Stretching ($\lambda_1 > 0$) and shrinking ($\lambda_1 < 0$) sheet geometry.

is first represented mathematically, and then it is numerically solved by applying the bvp4c technique. Figure 2 is shown to graphically depict the physical model. After that, a table and graphs representing the numerical results are produced. Since the model contains more than one solution, an assessment of stability is performed to determine which solution is stable. The impact of emerging factors on flow rates, concentration profiles, and transport of mass, including the Hartman number, Schmidt number, and destructive and generative chemical reaction parameters, are explored through graphs and tables.

While exploring the findings, we stumble upon the captivating existence of two possible solutions. In order to evaluate the feasibility and practicality of these solutions, an extensive analysis of stability was conducted. After conducting a comprehensive examination, we have reached a significant conclusion. It can be inferred that the first solution is the sole one that can be deemed stable and applicable in real-life situations. This statement is further reinforced by the detailed categorization and visual representation provided in Table 2 and Figure 3.

It is evident that the lowest eigenvalue moves toward zero as the value of γ near its critical point. This significant

Table 2: Smallest eigenvalues γ against λ_1

λ_1	γ	
	First solution	Second solution
−1.4429	0.00736	−0.00642
−1.440	0.06241	−0.2860
−1.436	0.28711	−0.3447
−1.4	0.48982	−0.5526

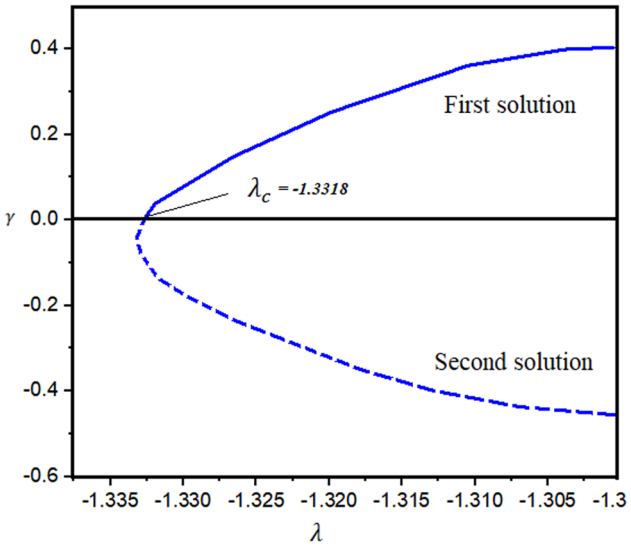

Figure 3: Smallest eigenvalues γ against λ.

discovery further supports the stability of the first solution by matching exactly with the findings of the stability study.

The pathways of the SMTr $C_0'(\eta)$ and $C_1'(\eta)$ for various values of Sc in relation to various quantities of M are shown in Figure 4a and b, while maintaining the same values for all the remaining variables. The numerical findings gathered from these graphs show that there is no resolution in the spectrum of $M_1 < M_{ci}$, whereas there could possibly be many solutions under a particular spectrum of $M_1 \geq M_{ci}$, $i = 1, 2, 3$. As shown in Figure 4a, M_{ci} stands for the critical amounts, which rise as the amounts of Sc increase from 0.3 to 0.9. The SMTr rises with increasing Sc enhances quantities. $M_{c1} = 0.21253$, $M_{c1} = 0.34211$, and $M_{c1} = 0.44421$ are the critical magnitudes for Sc = 0.3, 0.6, and 0.9, respectively. The chemical response factors at SMTr assorted λ are explained for γ_1, as shown in Figure 5a and b. According to the numerical findings, there are dual solutions in this situation as well. There are many solutions found in the spectrum $\lambda \geq \lambda_{ci}$, $i = 1, 2, 3$; no solutions found

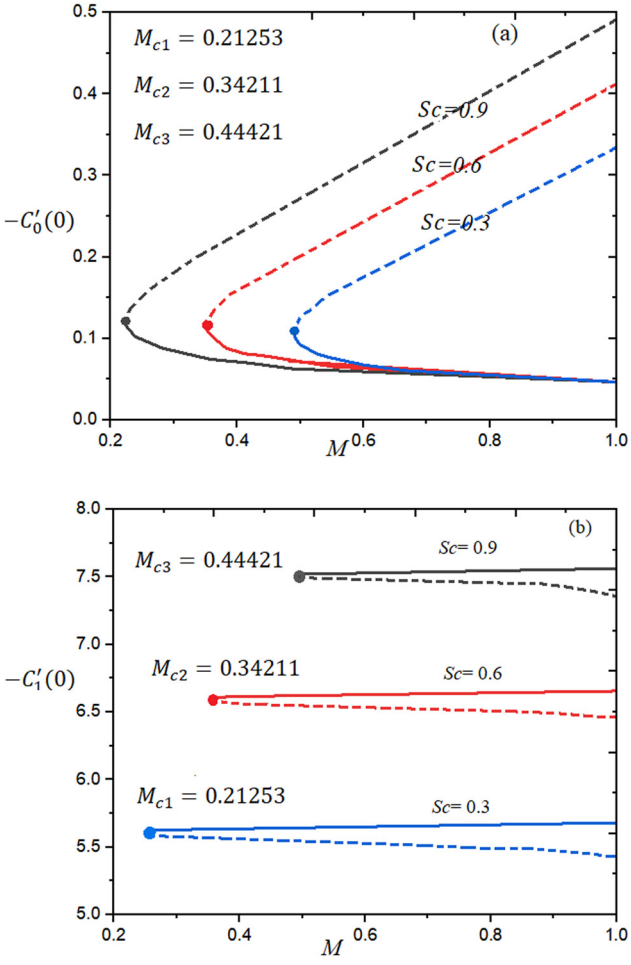

Figure 4: Variation of (a) $-C_0'(0)$ and (b) $-C_1'(0)$ for different values of Sc against M.

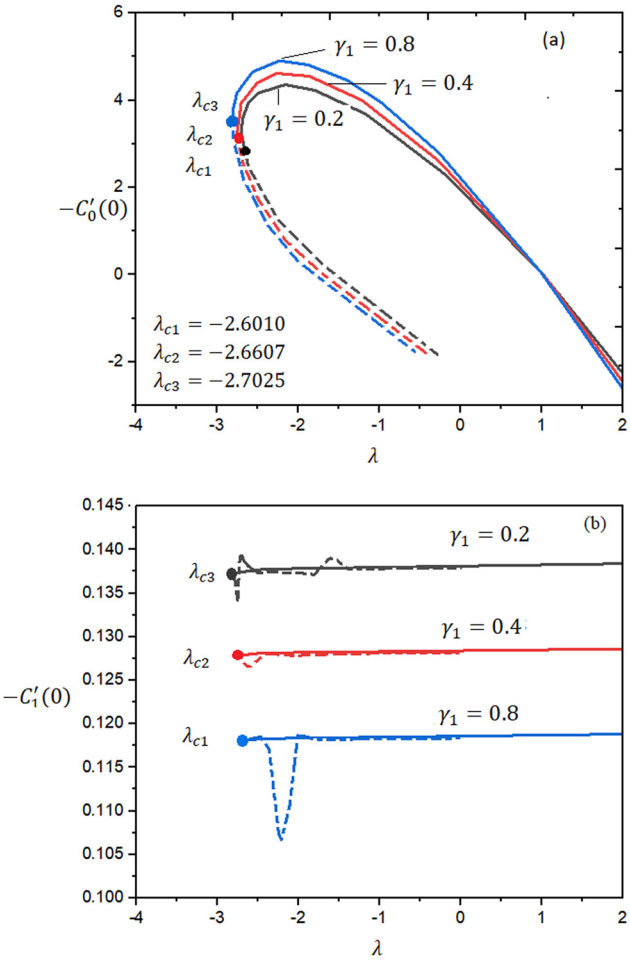

Figure 5: Variation of (a) $-C_0'(0)$ and (b) $-C_1'(0)$ for different values of γ_1 against λ.

in the region $\lambda < \lambda_{ci}$. As shown in Figure 5a and b, the critical quantities for γ_1 range from 0.2 to 0.8 and correspond to $\lambda_{c1} = -2.6010$, $\lambda_{c2} = -2.6607$, and $\lambda_{c3} = -2.7025$. For identical values of γ_1, which range from 0.2 to 0.8, it is found that $C_0'(\eta)$ increases while $C_1'(\eta)$ decreases. It is noteworthy to observe that Figure 5a shows dual behavior. The SMTr $C_0'(\eta)$ decreases in the vicinity of $-4 \le \lambda \le$, although it decreases in the region $1 < \lambda \le 2$. Deborah numbers $\Omega_1 = \Omega_2$ have an influence on SMTr against extending and contracting parameter λ, accordingly, as shown in Figure 6a and b. The decreasing functions of SMTr of $\Omega_1 = \Omega_2$ are examined. SMTr increases when the amount of $\Omega_1 = \Omega_2$ increases from 0.2 to 0.8, as seen in Figure 6a and b.

The impact of new variables on velocity components and SMTr, including Deborah numbers (DNs), Hartmann numbers (HNs), and Schmitt numbers (SNs), and generated and damaging chemical processes, is shown in Figures 7–24. The findings are shown in Figures 7 and 8, which show the

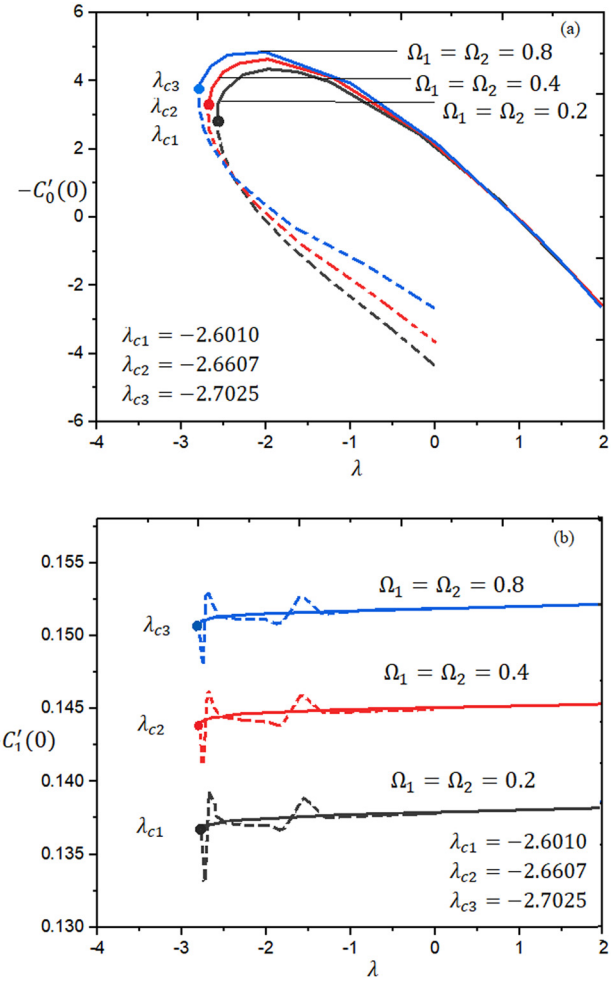

Figure 6: Variation of (a) $-C_0'(0)$ and (b) $-C_1'(0)$ for different values of $\Omega_1 = \Omega_2$ against λ.

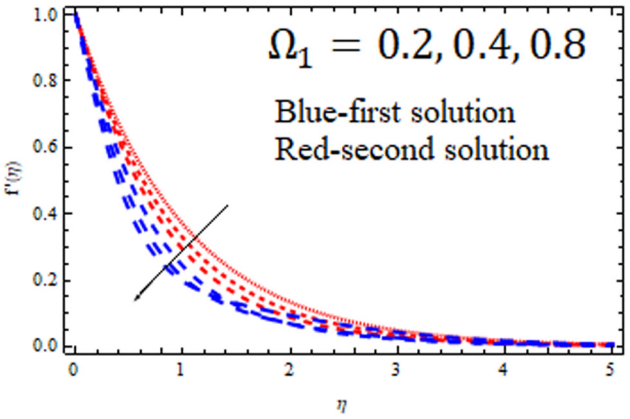

Figure 7: Effect of Ω_1 on f'.

various velocities profiles f' and g' that appear under various values of the DN. These profiles exhibit a noteworthy twin-branch feature that has been carefully examined. In particular, it is noticed that the velocity profiles show a falling trend over the boundary layer when the size of Ω_1 increases from 0.2 to 0.8.

It seems that Ω_2 has the opposite impact on velocity as Ω_1. Nonetheless, the fluid movement is improved with the dual solutions as the values of Ω_2 rise. Figures 11 and 12 show the relationship among the velocity coefficients and M, respectively. The velocity patterns show a declining trend as M values vary from 0.2 to 0.6. The addition of M to a fluid produces the drag force, sometimes referred to as the Lorentz force. The speed of the fluid across the boundary layer is slowed by this force.

The SMTr with distinct consequences of Ω_1 correspond to lower and higher solutions, as shown in Figures 13 and 14. It is investigated that SMTr rises with increasing levels of Ω_1. Figures 15 and 16 show how the SMTrr fluctuates as Ω_2 changes in magnitude. It is evident from Figures 15 and 16 that increasing Ω_2 causes SMTr to fall.

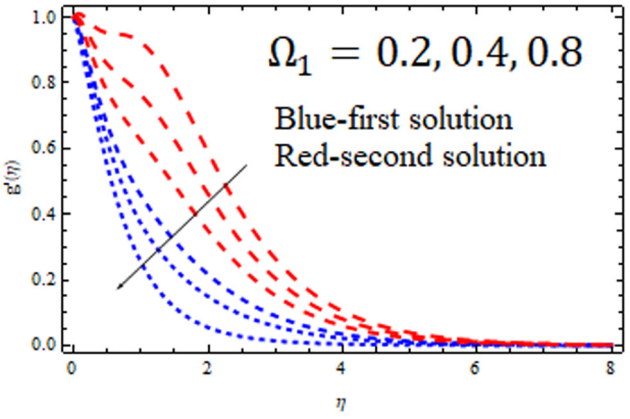

Figure 8: Effect of Ω_1 on g'.

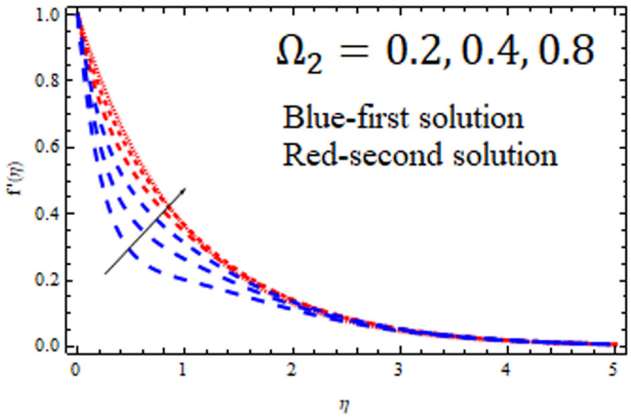

Figure 9: Effect of Ω_2 on f'.

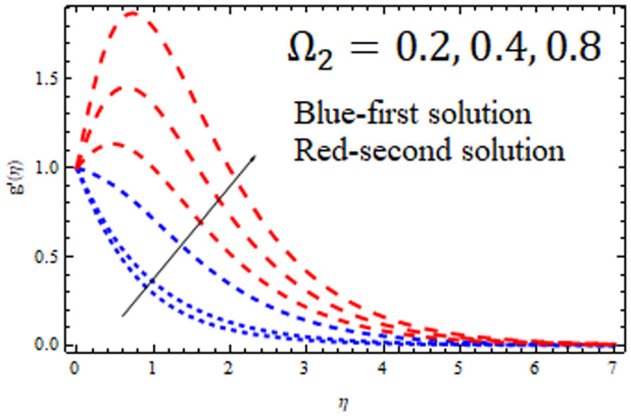

Figure 10: Effect of Ω_2 on g'.

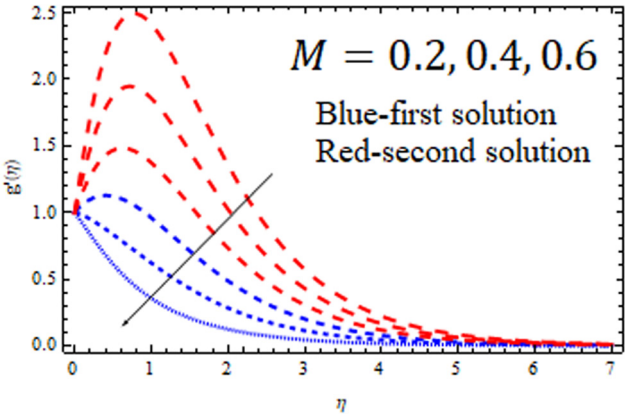

Figure 12: Effect of M on g'.

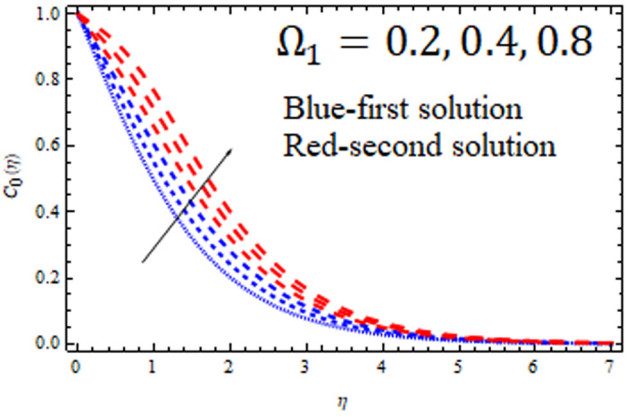

Figure 13: Effect of Ω_1 on C_0.

For all scenarios, a rising trend in the SMTr is predicted as the amount of M rises from 0.2 to 0.5 (Figures 17 and 18). Comparable to a drag force, the Lorentz force is a restricting force that arises when M exists. This force reduces the liquid's velocity by opposing its movement. As a result, there is an increase in SMTr, which significantly stimulates convection forces as well as energy transference. Furthermore, in both methods, the thermodynamic boundary region layer's thickness is increased.

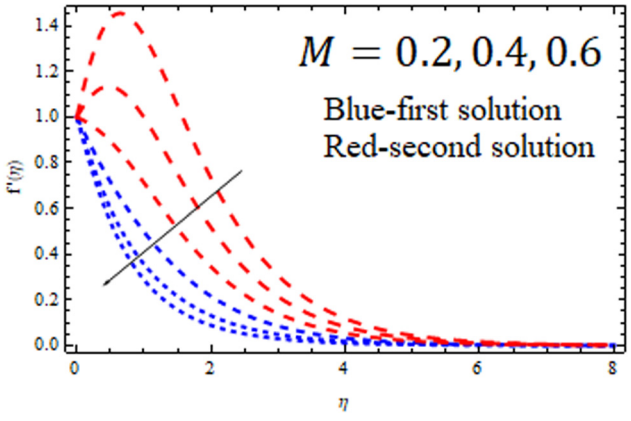

Figure 11: Effect of M on f'.

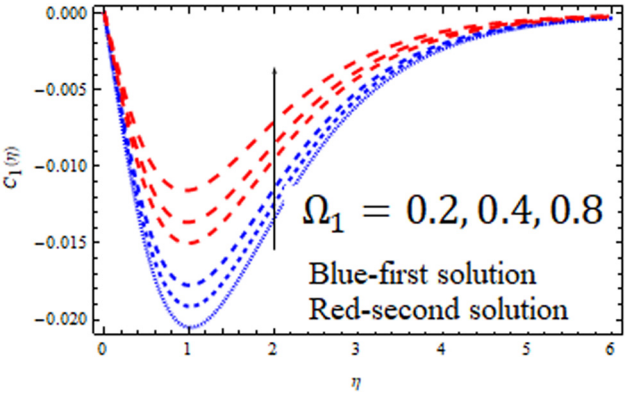

Figure 14: Effect of Ω_1 on C_1.

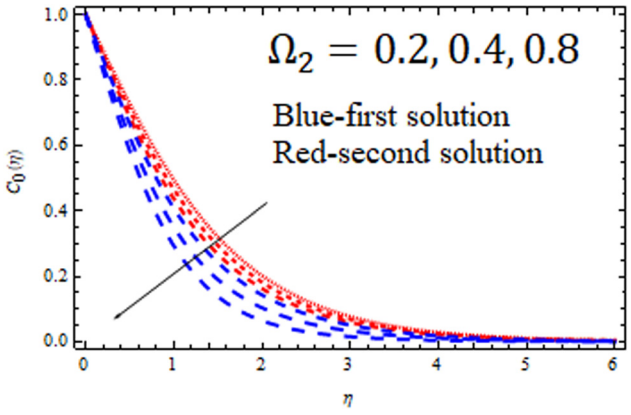

Figure 15: Effect of Ω_2 on C_0.

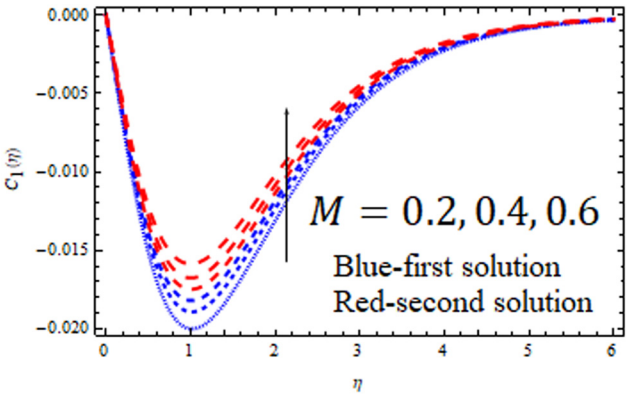

Figure 18: Effect of M on C_1.

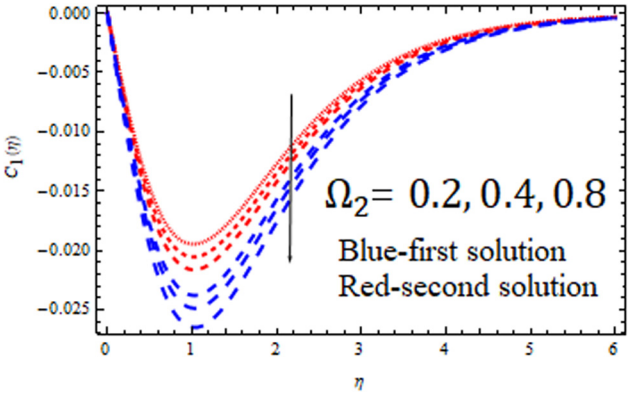

Figure 16: Effect of Ω_2 on C_1.

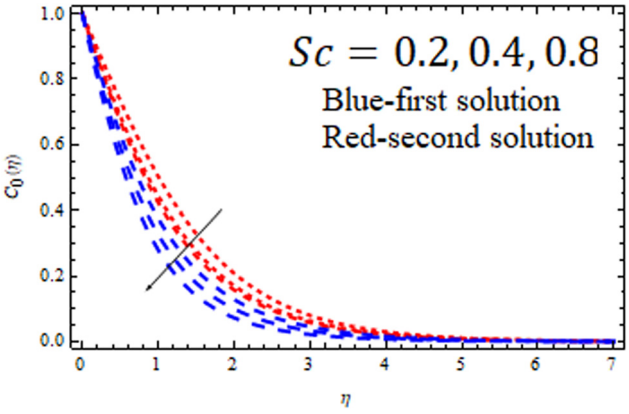

Figure 19: Effect of Sc on C_0.

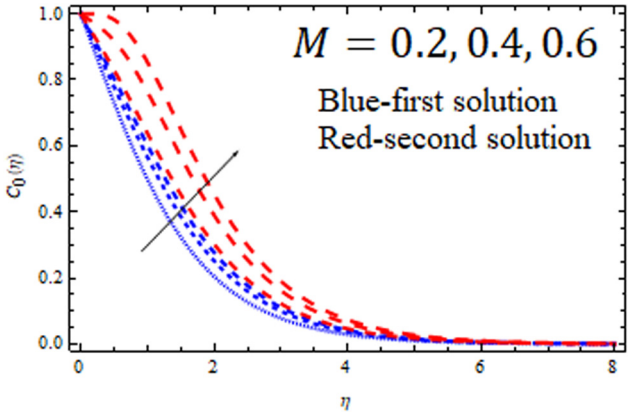

Figure 17: Effect of M on C_0.

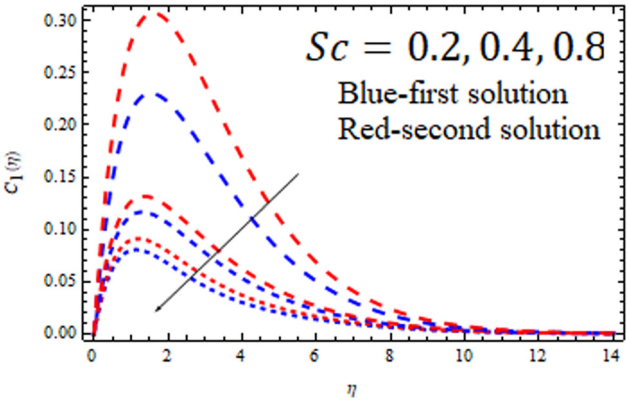

Figure 20: Effect of Sc on C_1.

Figures 19 and 20 show how SMTr is affected by the SN. In both instances, the SMTr reduces as Sc increases in strength. There is a more obvious difference between the primary and second solutions. The impact of both productive and destroying chemical processes on the SMTr is shown in Figures 21–24 appropriately. Figures 21 and 22 show that SMTr responds to destroying chemical processes with a decreasing trend, while Figures 23 and 24 show that SMTr responds to productive chemical processes with a rising pattern.

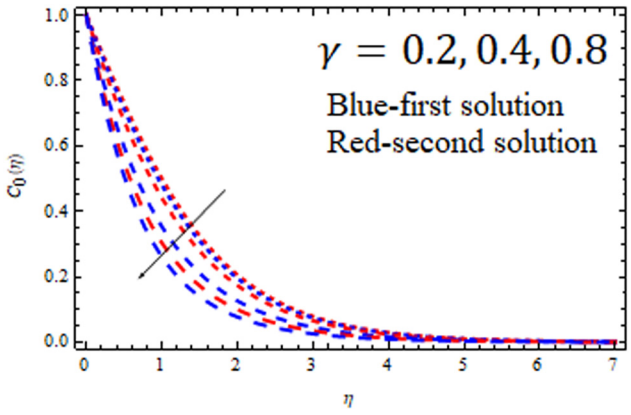

Figure 21: Effect of γ on C_0.

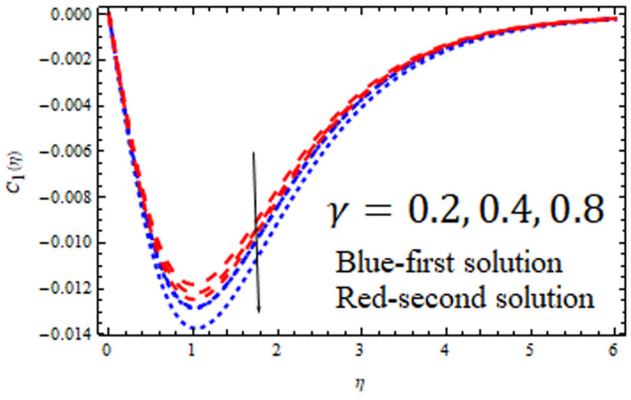

Figure 22: Effect of γ on C_1.

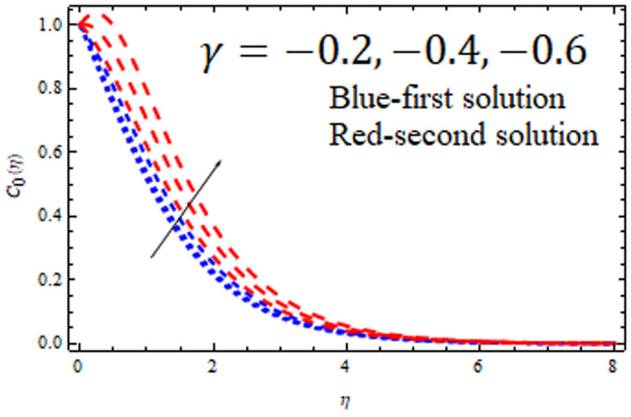

Figure 23: Effect of $\gamma(<0)$ on C_0.

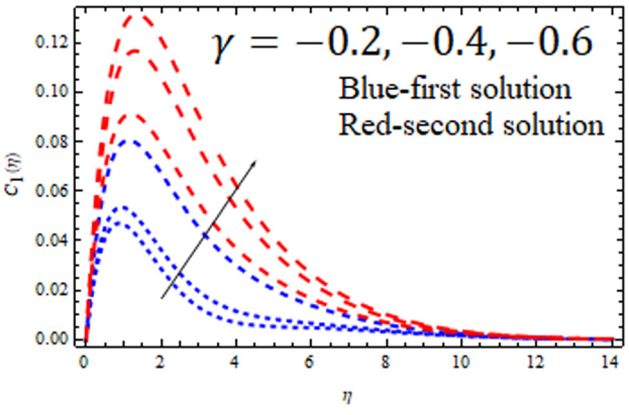

Figure 24: Effect of $\gamma(<0)$ on C_1.

5 Conclusions

The behavior of a 2D MHD Jeffery fluid flow model over an exponentially shrinking surface beneath the effect of generative and destructive chemical processes is described numerically in the current investigation. By resemblance alteration, the fundamental flow models are transformed from partial differential equations to ODEs. Using bvp4c, the computational solution for the SMTr and velocity is derived. This work is genuinely novel in that it carefully investigates the effects and durability of the Lorentz force on Jeffery fluid, especially when it comes to either expanding or contracting surfaces that undergo internal exchange of heat and both productive and destructive chemical processes.

It is noteworthy that there has not been a thorough analysis of this kind in the literature that has already been written about this topic. As a result, the previously released research validates the current work. A thorough stability study is performed to guarantee the system's stability, and the results show that the first option is trustworthy. The investigation's numerical findings show that there are many solutions in the spectrum $M_1 \geq M_{ci}$, $i = 1, 2, 3$; and that there is only one solution in the domain $M_1 < M_{ci}$. The critical amounts, represented by M_{ci}, rise as the amounts of Sc increase from 0.3 to 0.9. Comparably, we find that there are many resolutions in the spectrum $\lambda \geq \lambda_{ci}$, $i = 1, 2, 3$, and none in the vicinity $\lambda < \lambda_{ci}$. The thresholds for γ_1 vary between 0.2 and 0.8, and they correspond to $\lambda_{c1} = -2.6010$, $\lambda_{c2} = -2.6607$, and $\lambda_{c3} = -2.7025$. A decreasing trend is predicted between SMTr and DN. It is seen that the velocity curves show a diminishing trend over the boundary layer when the size of Ω_1 grows from 0.2 to 0.8. For the velocity characteristics, a declining behavior is shown as the M increases from 0.2 to 0.6. We find that SMTr responds to destroying chemical processes with a decreasing trend, while SMTr responds to generative chemical processes with a rising pattern.

Acknowledgments: The authors extend their appreciation to Taif University, Saudi Arabia, for supporting this work through project number (TU-DSPP-2024-87).

Funding information: This research was funded by Taif University, Saudi Arabia, project No. TU-DSPP-2024-87.

Author contributions: Conceptualization, A.A and Zeeshan; data curation, M.A; data fitting, M.A; modeling, M.A; data interpretation, M.A; methodology, A.A. and N.I.; software M.A and Zeeshan; validation, N.I, R.S., and Zeeshan.; simulation, M.A; formal analysis, M.A.; investigation, N.I, R.S., and Zeeshan.; writing – original draft preparation, Zeeshan and R.S.; writing – review and editing, M.A. and R.S.; validation, M.A, visualization, Zeeshan. and M.A. All authors have accepted responsibility for the entire content of this manuscript and approved its submission.

Conflict of interest: The authors state no conflict of interest.

Data availability statement: The datasets generated and/or analysed during the current study are available from the corresponding author on reasonable request.

References

[1] Sakiadis BC. Boundary-layer behavior on continuous solid surfaces: I. Boundary-layer equations for two-dimensional and axisymmetric flow. AIChE J. 1961;7(1):26–8.

[2] Sun L, Wang G, Zhang C. Experimental investigation of a novel high performance multi-walled carbon nano-polyvinylpyrrolidone/silicon-based shear thickening fluid damper. J Intell Mater Syst Struct. 2024;35(6):661–72.

[3] Krishna CM, ViswanathaReddy G, Souayeh B, Raju CSK, Rahimi-Gorji M, Raju SSK. Thermal convection of MHD Blasius and Sakiadis flow with thermal convective conditions and variable properties. Microsyst Technol. 2019;25:3735–46.

[4] Wang Z, Zhao Q, Yang Z, Liang R, Li Z. High-speed photography and particle image velocimetry of cavitation in a Venturi tube. Phys Fluids. 2024;36(4):045147.

[5] Zhu C, Al-Dossari M, Rezapour S, Gunay B. On the exact soliton solutions and different wave structures to the (2+1) dimensional Chaffee–Infante equation. Results Phys. 2024;57:107431.

[6] Han T, Cao W, Xu Z, Adibnia V, Olgiati M, Valtiner M, et al. Hydration layer structure modulates superlubrication by trivalent La3 + electrolytes. Sci Adv. 2023;9(28):eadf3902. doi: 10.1126/sciadv.adf3902.

[7] Hayat T, Abbas Z, Ali N. MHD flow and mass transfer of a upper-convected Maxwell fluid past a porous shrinking sheet with chemical reaction species. Phys Lett A. 2008;372(26):4698–704.

[8] Hayat T, Sajid M, Pop I. Three-dimensional flow over a stretching surface in a viscoelastic fluid. Nonlinear Anal: Real World Appl. 2008;9(4):1811–22.

[9] Alizadeh-Pahlavan A, Sadeghy K. On the use of homotopy analysis method for solving unsteady MHD flow of Maxwellian fluids above impulsively stretching sheets. Commun Nonlinear Sci Numer Simul. 2009;14:1355.

[10] Ariel PD, Hayat T, Asghar S. The flow of an elastico-viscous fluid past a stretching sheet with partial slip. Acta Mech. 2006;187(1):29–35.

[11] Vajravelu K. Viscous flow over a nonlinearly stretching sheet. Appl Math Comput. 2001;124(3):281–8.

[12] Vajravelu K, Cannon JR. Fluid flow over a nonlinearly stretching sheet. Appl Math Comput. 2006;181(1):609–18.

[13] Cortell R. Effects of viscous dissipation and radiation on the thermal boundary layer over a nonlinearly stretching sheet. Phys Lett A. 2008;372(5):631–6.

[14] Cortell R. Viscous flow and heat transfer over a nonlinearly stretching sheet. Appl Math Comput. 2007;184(2):864–73.

[15] Hayat T, Abbas Z, Javed T. Mixed convection flow of a micropolar fluid over a non-linearly stretching sheet. Phys Lett A. 2008;372(5):637–47.

[16] Raptis A, Perdikis C. Viscous flow over a non-linearly stretching sheet in the presence of a chemical reaction and magnetic field. Int J Non-Linear Mech. 2006;41(4):527–9.

[17] Das S, Jana RN, Makinde OD. MHD flow of Cu-Al2O3/water hybrid nanofluid in porous channel: Analysis of entropy generation. Defect Diffus Forum. 2017;377:42–61. doi: 10.4028/www.scientific.net/DDF.377.42.

[18] Wahid NS, Arifin NM, Turkyilmazoglu M, Hafidzuddin MEH, Abd Rahmin NA. MHD Hybrid Cu-Al2O3/water nanofluid flow with thermal radiation and partial slip past a permeable stretching surface. Anal Solution J Nano Res. 2020;64:75–91. doi: 10.4028/www.scientific.net/JNanoR.64.75.

[19] Chu YM, Khan MI, Waqas H, Farooq U, Khan SU, Nazeer M. Numerical simulation of squeezing flow Jeffrey nanofluid confined by two parallel disks with the help of chemical reaction: effects of activation energy and microorganisms. Int J Chem React Eng. 2021;19(7):717–25.

[20] Lund LA, Omar Z, Dero S, Chu Y, Khan I. Temporal stability analysis of magnetized hybrid nanofluid propagating through an unsteady shrinking sheet: Partial slip conditions. Computers Mater Continua. 2020;66(2):1963–75.

[21] Khan MI, Kadry S, Chu YM, Khan WA, Kumar A. Exploration of Lorentz force on a paraboloid stretched surface in flow of Ree-Eyring nanomaterial. J Mater Res Technol. 2020;9(5):10265–75.

[22] Souayeh B, Yasin E, Alam MW, Hussain SG. Numerical simulation of magnetic dipole flow over a stretching sheet in the presence of non-uniform heat source/sink. Front Energy Res. 2021;9:767751.

[23] Souayeh B. Simultaneous features of CC heat flux on dusty ternary nanofluid (Graphene+Tungsten oxide+Zirconium oxide) through a magnetic field with slippery condition. Mathematics. 2023;11(3):554.

[24] Shampine LF, Gladwell I, Thompson S. Solving ODEs with MATLAB. 1st edn. Cambridge: Cambridge University Press; 2003.

[25] Tasawar H, Muhammad Q, Zaheer A, Hendid AA. Magnetohydrodynamic flow and mass transfer of a Jeffery fluid over a nonlinear stretching surface. Z Naturforsch. 2010;65a:1111–20.